6. International conference on spectral line shapes
Boulder, CO, USA 7 - 12 Jul 1982
CEA-CONF--6438

SUITABLE SPECTRAL LINE SHAPE CALCULATIONS FOR INERTIAL CONFINEMENT PLASMA DIAGNOSIS

D. Lambert, M. Louis-Jacquet

Commissariat à l'Energie Atomique, Centre d'Etudes de Limeil
B.P. n° 27, 94190 Villeneuve-Saint-Georges

1. Introduction

An ideal diagnosis for dense plasmas should include time-and-space-resolved analysis of density and temperature parameters. And this all the time of complete plasma evolution long. In plasma confinement experiments, however, the knowledge of the plasma state at the maximum compression time would yet be of utmost interest. For quite many experiments, this time can correspond to a stationnary state during which the X emission conditions for a moderate Z element are maximum.

If one can get rid of spatial analysis by use of a geometrically confined emitting element (such as a heavy gas inside a microballoon the wall of which bears the gradients due to laser-matter interaction), and one can assume by calculating the emissivity in a given bandwidth that the radiated energy will be mostly delivered during the stationnary step, then the time and space integrated spectroscopic diagnosis will provide a tolerably equivalent mean to the ideal time and space resolved diagnosis. For laser inertialy confined plasmas, this happens to be nearly true.

Since this diagnosis mean deals with emission only, we need to get rid of reabsorption problems, since their calculation depends on the use of an ionization-excitation plasma model. That is the reason why we will focus our attention onto the aspects of spectroscopic theory which control the low reabsorption line shapes - from high values of n - and more precisely the lesser reabsorbed parts of the line shapes - the wings instead of the center -.

2. Parameters magnitude in laser plasmas

In laser confinement experiments, most plasmas present the following features : temperature between 30 and 1000 eV, and electrons density between 10^{21} and 10^{24} cm^{-3}. These values will determine the time orders of magnitude for the different perturbation phenomena. If one calculates the characteristic time as the ratio of the mean distance between particles to their thermal speed, one finds :

for Ne^{X} or Ar^{XVIII} ions	$t > 10^{-15}$ s
for light ions D^+, T^+	$3\ 10^{-14} > t > 3\ 10^{-16}$ s
for electrons	$4\ 10^{-16} > t > 6\ 10^{-18}$ s

For electrons, the mean distance between particles is more significative of electron-electron collision processes than of the electron-ion phenomena modifying the ionic X emission. One should therefore replace this distance by the mean orbital radius of the ion optical electron. Then

for $Neon^{X}$	n = 1	$1.5\ 10^{-18} > t > 2.5\ 10^{-19}$
	n = 4	$2.5\ 10^{-17} > t > 4.5\ 10^{-18}$
for $Argon^{XVIII}$	n = 1	$8.5\ 10^{-19} > t > 1.5\ 10^{-19}$
	n = 4	$4.5\ 10^{-17} > t > 2.5\ 10^{-18}$

These values $t > 10^{-15}$ s for medium Z ions and $5\ 10^{-17} > t > 2.5\ 10^{-19}$ s for electrons are to be compared with the radiation period (from 10^{-18} s for Ar^{XVIII} Lyman α to $4\ 10^{-15}$ s for Ne^{X} Lyman α) and the coherence time of such a photon, about 10^{3} - 10^{5} times the radiation period. The same values must also be compared to the Heisenberg time associated with energy width. For energy spreading in the range 1 eV to 100 eV, the limits of the associated time are $4\ 10^{-15}$ s and $4\ 10^{-17}$ s.

Let us review these three kinds of characteristic times, and their implications over the perturbations treatment. First, the ionic interaction time is so large (10^{-15} s) that the quasistatic treatment is perfectly correct. Second, the electronic interaction time is so short that the impact approximation is correct as long as the electronic temperature is over 100 eV, so that $t < 10^{-17}$ s. Third, by dynamical effects, light ions D^+ and T^+ interactions with Ne^{X} or Ar^{XVIII} emitter belong to an intermediary zone for which the impact and quasistatic approximations are false.

The model should be correct only for energy spreading so large ($\Delta W \sim 100$ eV) that the signal to noise ratio becomes too bad for a diagnosis. Consequently, we will study the Stark broadening effects on middle Z hydrogenic ions line shapes only, and focus our attention over the quasistatic effects.

3. Spectral emission

For a transition from the state $|i\rangle$ to the state $|f\rangle$ the emitting power (1) is

$$P(\omega) = \text{Trace}\ \rho\, \delta(\omega - \omega_{if})\, \underset{|i\rangle\ |f\rangle}{J}(\omega)$$

$$\underset{|i\rangle\ |f\rangle}{J}(\omega) = \frac{\omega_{if}^4}{3\pi\varepsilon_0 c^3} \left\| \langle i | \vec{d} | f \rangle \right\|^2$$

$$\hbar\omega_{if} = W_i - W_f$$

where ρ is the total density operator, $\hbar\omega_{if}$ is the energy difference between states $|i\rangle$ and $|f\rangle$ and $\vec{d}$ the dipolar momentum operator. One should notice this dipolar emission expression is valid as long as the wavelength is larger than the dipolar length

$$\lambda \gg \left\| \langle i | \frac{\vec{d}}{q} | f \rangle \right\|$$

This has been verified in our calculation.

The trace over the density operator corresponds to a summation over the whole configurations set since,- as we use quasistatic hypothesis - the evolution of a perturbing phenomenon cannot be represented but by a probability of distinct configurations. To sum over the density operator, one needs probability distribution of the various global configurations. These configurations must include the state of the inner system - ion nucleus plus optical electron in H like emission - but also the state of the rest of the universe - mainly the rest of the plasma -. Since the

perturbation is created by other particles the electromagnetic interaction of which is a long range one, any hope to describe the configuration by a detailed position of the perturbers is irrealistic. We agree to depict representations distribution by the simple probability of the microfield at the center of the emitter nucleus. This distribution itself is given by the first part of Boltzman probability expansion - as well in Baranger-Mozer (2) as in Hooper and Tighe (3).

Up to now, the tabulated P(F) microfield distributions deal with a fixed emitter (which is compatible with all the hypothesis), the self consistant state is not taken into account. Then, the particular state $|i\rangle$ of the emitter is of no influence over the perturbers distribution and then on the microfield probability distribution. Thus a real hierarchy is created among the two sub-systems, the perturbers distribution - represented by the microfield - fixing the eigen state $|i\rangle$ without any back effect of $|i\rangle$ on $\mathcal{P}(\vec{F})$. Since any symetry direction of $|i\rangle$ cannot react on $\mathcal{P}(\vec{F})$, the microfield probability $\mathcal{P}(\vec{F})$ can be replaced by the microfield modulus probability $\mathcal{P}(F)$. If one wants to describe the field around the emitter nucleus, and to describe the inhomogeneity of the microfield at the emitter (nucleus plus electron) system scale, one needs further hypothesis - about the nearest perturbers, at least - to determine a probability distribution including the microfield spatial derivatives. Due to the hierarchy (plasma representation $F \Rightarrow |i\rangle$) the trace summation is factorizable

$$\text{Trace } \rho = \int dF\, \mathcal{P}(F) \otimes \text{Trace } \rho_{|i\rangle}$$

and even

$$\text{Trace } \rho = \int dF \left[\mathcal{P}(F) \otimes \text{Trace } \rho_{|i\rangle} \right]$$

To each value F of the microfield corresponds the set of the eigen energies $\{W_i\}$ of the eigenstates $\{|i\rangle\}$. This allows to perform the summation of the part of the density operator restricted to the eigen states of the emitter only.

A further simplification is even common. For each value of the microfield F, the diagonal term corresponding to $|i_o\rangle$ in the density operator matrix is

$$\mathcal{P}_{|i_o\rangle} = \frac{g_{i_o}\, e^{-\frac{W_{i_o}}{k_B T_e}}}{\sum_i g_i\, e^{-\frac{W_i}{k_B T_e}}}$$

Most calculations treat only one line shape at one time, so the energy differences from one part to an other are only a small fraction of the line mean energy. Thus, the influence of Boltzman terms is low and the term ω_{if}^4 in the power expression is nearly constant. The diagonal term can be approximated by

$$\omega_{if}^4 \frac{g_i\, e^{-\frac{W_i}{k_B T_e}}}{Z} |i\rangle\langle i| \sim K\, g_i |i\rangle\langle i|$$

where K is a constant (without interest in the usual arbitrary units) and Z the partition function. This leads to

$$J(\omega) = \sum_{|j\rangle} \int dF\, \mathcal{P}(F) \left\| \langle j_{(F)}| \vec{d} |i\rangle \right\|^2 \delta(\omega - \omega_{ij})$$

the so called "line profile" where $|j\rangle$ is an eigen state corresponding to the value F of the integration. We can use this expression as long as we determine only an isolated line, which means we forget all interactions between the level n and any other $n' \neq n$. To restore the spectrum, one needs to add the different line shapes multiplied by a coefficient corresponding to the precise energy of each line. This means summing the various $\mathcal{P}_{|io\rangle}$ over the different $|io\rangle$ originating from each precise line. On the contrary, we present in this paper the calculation of the eigen energies and the eigen states after including the terms $n \neq n'$, which corrects a former systematic error. Then, to get the self consistant whole spectrum calculation, we need to use the original power expression $\mathcal{P}(\omega)$. This will

be presented in a further paper. As a remark, one can notice that the use of Boltzman probability is not a theoretical obligation and should be replace by a detailed atomic balance in non LTE at least. But the calculation is still complicated enough with Boltzman's !

4. Quasistatic perturbations expression

The separation between slow phenomena associated to ions and quick electronic collisions settles the problem of individual actions of electrons as they are treated outside of the quasistatic resolution. But there exists a collective electronic effect, statistically evident as it insures the quasi neutrality of the plasma. So the ionic perturbers are screened by the statistical low frequency effect of electrons and the quasistatic perturbation is

$$H = H_0 - qV$$

$$V = \sum_p \frac{Z_p q}{4\pi\varepsilon_0 \|\vec{R}_p - \vec{r}\|} e^{-\frac{\|\vec{R}_p - \vec{r}\|}{\lambda}}$$

where p represents the ionic perturbers, R_p the distance of each one to the center of the emitting ion O, and r is the location parameter refering to the same point O. This kind of potential is used in both calculations of Baranger-Mozer or Hooper-Tighe to determine $\vec{F}$ (F) and thus the calculation is self consistant. The calculation of the eigen solutions needs the determination of the perturbation matrix coefficients which means an integration of V over $\vec{r}$ for the whole space - at least for the whole region where the projection states we use (the spherical solution of hydrogenoid ion) have a large electronic probability. Even in that restricted volume (mainly $||\vec{r}||$ less than a few $\frac{a_0}{Z} n^2$) the density reached by laser plasmas experiments makes the field F far from constant. Since there is no correlated probability distribution of both the field and its many space derivatives, one needs a further hypothesis about the field space variation.

5. The first nearest neighbourg (1NN) approximation

The expression of the perturbation potential

$$V = \sum_p \frac{Z_p q}{4\pi\varepsilon_0 \|\vec{R}_p - \vec{r}\|}$$

includes the perturbers distance

$$R_p = \sqrt{\frac{Z_p q}{4\pi\varepsilon_0 F_p}}$$

calculated from the value of the individual microfield F_p assuming there is no screening. With the screened potential

$$V = \sum_p \frac{Z_p q}{4\pi\varepsilon_0 \|\vec{R}_p - \vec{r}\|} e^{-\frac{\|\vec{R}_p - \vec{r}\|}{\lambda}}$$

R_p is only determined by the implicit equation

$$F_p = \frac{-Z_p q}{4\pi\varepsilon_0 \|\vec{R}_p - \vec{r}\|} \left(\frac{1}{\|\vec{R}_p - \vec{r}\|} + \frac{1}{\lambda}\right) e^{-\frac{\|\vec{R}_p - \vec{r}\|}{\lambda}}$$

for which a numerical solution would be easy for each value of F_p. But the problem is we only know the vectorial sum $\vec{F}$ and not the individual components

$$\vec{F} = \sum_p \vec{F}_p$$

So the simplest hypothesis is to consider the vectorial sum as a single component, that is to assume that the total field is created by the first nearest perturber only, the contributions of the other ones statistically vanishing, or being considered as relevant of a further order of approximation. The restriction to one perturber only results into the particularization of its direction from the emitting ion. So the screening cloud of electrons cannot be homogeneous nor isotropic, and the expression of screened potential can no longer be correct. So we have the choice of a false expression of screened potential and a simpler false expression of simple ion potential. We choose that last since we are sure not to take the electronic effect into account twice by the further electronic impact

treatment, and since we can lower the error by using an effective Z_p instead of Z_p.

6. INN Quasistatic treatment

Using the previous formulas

$$H = H_0 - \frac{Z_p q^2}{4\pi\varepsilon_0 \|\vec{R}_p - \vec{r}\|}$$

$$R_p = \sqrt{\frac{Z_p q}{4\pi\varepsilon_0 F}}$$

$$\vec{R}_p = R_p \vec{k} \qquad \vec{k} // Oz$$

we can develop the perturbation by using

$$\frac{1}{\|\vec{R}_p - \vec{r}\|} = \sum_i^{\infty} \frac{1}{Max\{R_p, r\}} \left[Min\left\{\frac{r}{R_p}, \frac{R_p}{r}\right\}\right]^i Y_i^0(\theta,\varphi)$$

Space must be parted in two regions

$$r > R_p \Rightarrow \frac{1}{\|\vec{R}_p - \vec{r}\|} = \frac{1}{r} \sum_i \left(\frac{R}{r}\right)^i Y_i^0(\theta,\varphi)$$

$$R_p > r \Rightarrow \frac{1}{\|\vec{R}_p - \vec{r}\|} = \frac{1}{R_p} \sum_i \left(\frac{r}{R_p}\right)^i Y_i^0(\theta,\varphi)$$

the inside and the outside of the sphere centered on the emitter and of radius R_p. Yet, even with the reduced density operator $g_i|i><i|$ inside the line profile expression, the elements of the hamiltonian matrix

$$H = H_0 + \sum_i V_i$$

are determined by the integration over the optical electron space. Since we want it to keep in bound state and will use only bound projection states, the inside of the sphere must be the most important probability-of-existence region. Then we use the expression developped in powers of $(\frac{r}{R_p})$ and not of $(\frac{R_p}{r})$, while integrating over the whole space $0 < r < \infty$. The interest of using a single expression for the whole space is the possibility of an exact arithmetic calculation of the integration (4).

Then we have

$$H = H_o + \sum_i V_i$$

$$\langle n\ell m | V_i | n'\ell'm' \rangle = -\frac{Z_p q^2}{4\pi\varepsilon_o R_p} \langle n\ell m | \left(\frac{r}{R_p}\right)^i Y_i^0(\theta,\varphi) | n'\ell'm' \rangle$$

Of course we must make sure after the determination of the eigenstates that $\langle r \rangle \ll R_p$ is verified.

The diagonalization of the hamiltonian operator $H = H_o + \sum_i V_i$ is the only method to get the exact eigen energies and eigenstates. But then the diagonalization needs to be effected using a complete basis of projection states. The complete set of spherical solutions of hydrogenoïd atom not only includes the discrete infinity of bound states but also the continuum of free states. Any diagonalization over a complete set is then impossible. But we can at least use the least incomplete set the computer can accept. As we are interested, for diagnosis purpose, in the lines α and γ from levels 3 and 4, we have proceeded to the diagonalization over the states originating from the levels n = 1, 2, 3, 4 and 5, which means we will deal with perturber terms V_1 to V_8 since

$$i > n + n' - 2 = \text{Max}(\ell' + \ell)$$

$$\Rightarrow \langle n\ell m | Y_i^0(\theta,\varphi) | n'\ell'm' \rangle = 0$$

To check the effect of near by levels, we have effected the calculations twice. First we used only the terms of a source level, that is only $\langle n\ell m | V_i | n\ell'm' \rangle$. Then we included the terms $\langle n\ell m | V_i | n'\ell'm' \rangle$ with $n' \neq n$. In order to make the demonstration clearer, we used the expedient of exagerating the effect of $n' \neq n$ terms by multiplying all of them by an arbitrary factor, adjustable from very small values (to demonstrate the effect of existence by itself) up to a few units (for example to follow the progression of energy deformation and better understand the intersection - see infra -).

It has yet been pointed that Oz direction is now a symmetry axis. So the magnetic moment projection M_z is a constant, and all terms connecting

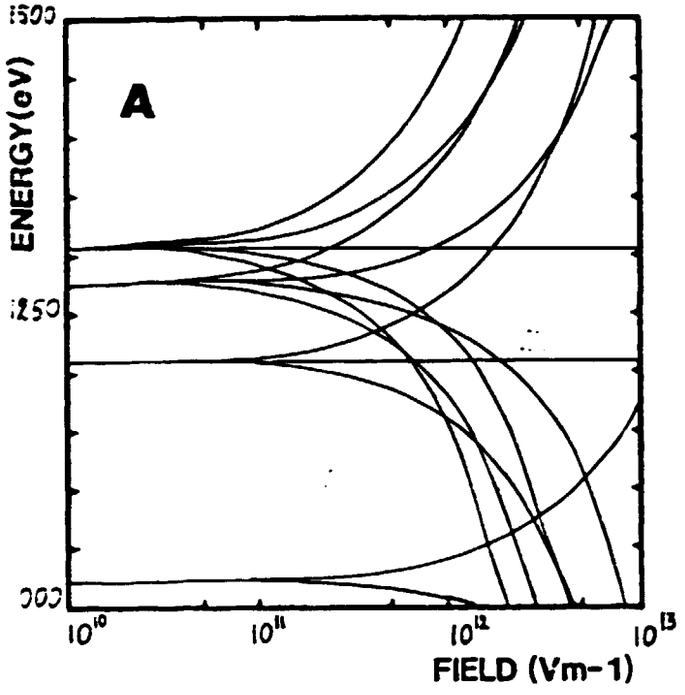
A
ENERGY(eV)
FIELD (Vm-1)

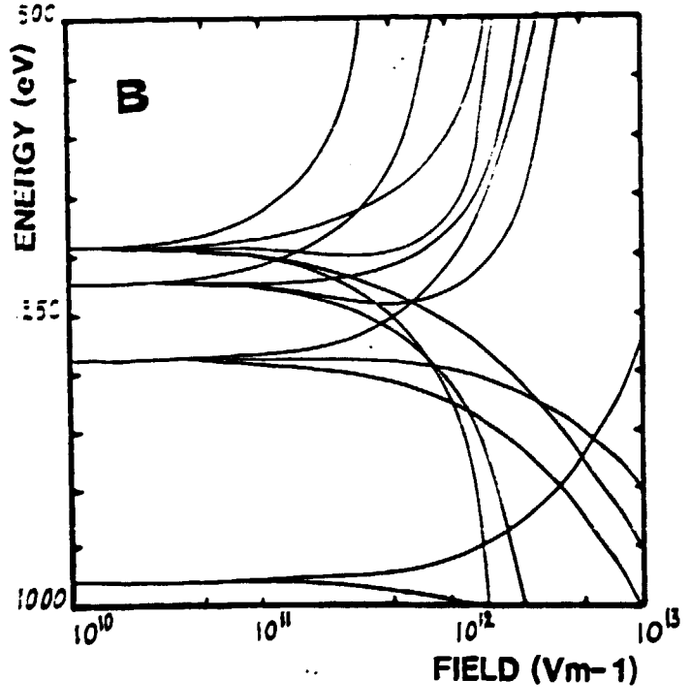
B
ENERGY (eV)
FIELD (Vm-1)

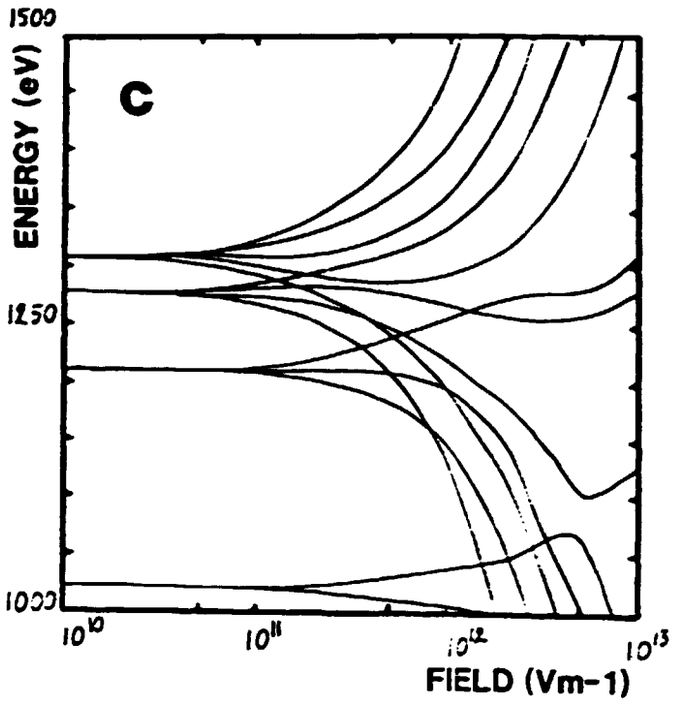

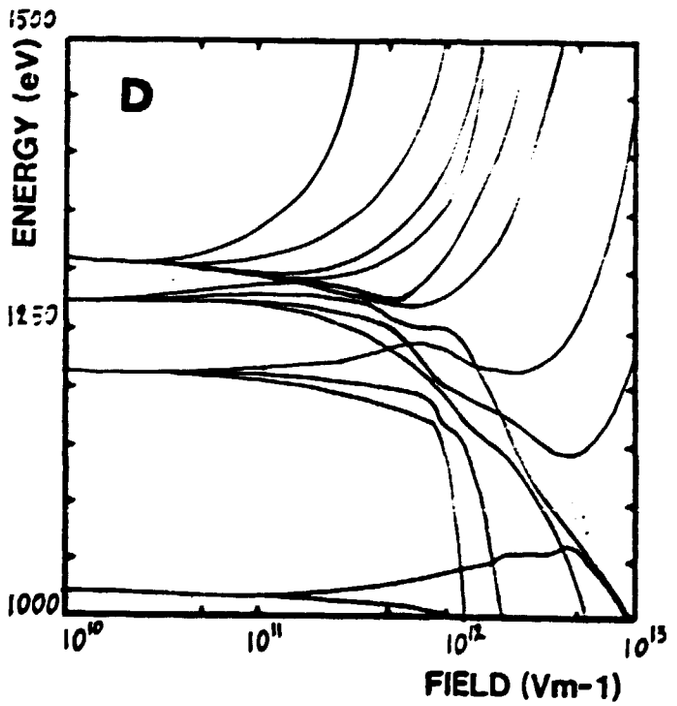

Fig. 1 : Energy splitting by a single perturber for the m = 0 states.
A and B deal with n = n' perturbation terms only, C and D with all n' ≠ n
A and C deal with linear perturbing term only, B and D will all the V_i

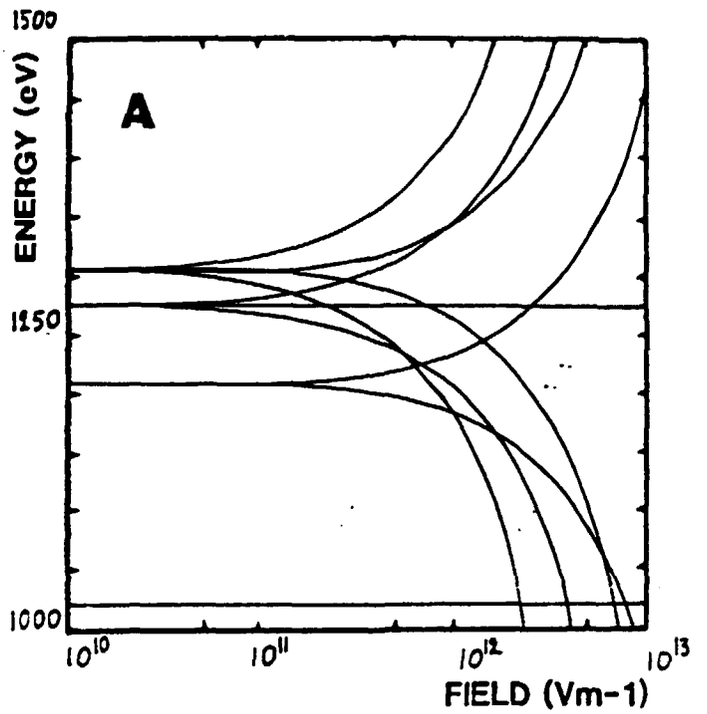
1500
ENERGY (eV)
A
1250
1000
10^{10}
10^{11}
10^{12}
10^{13}
FIELD (Vm-1)

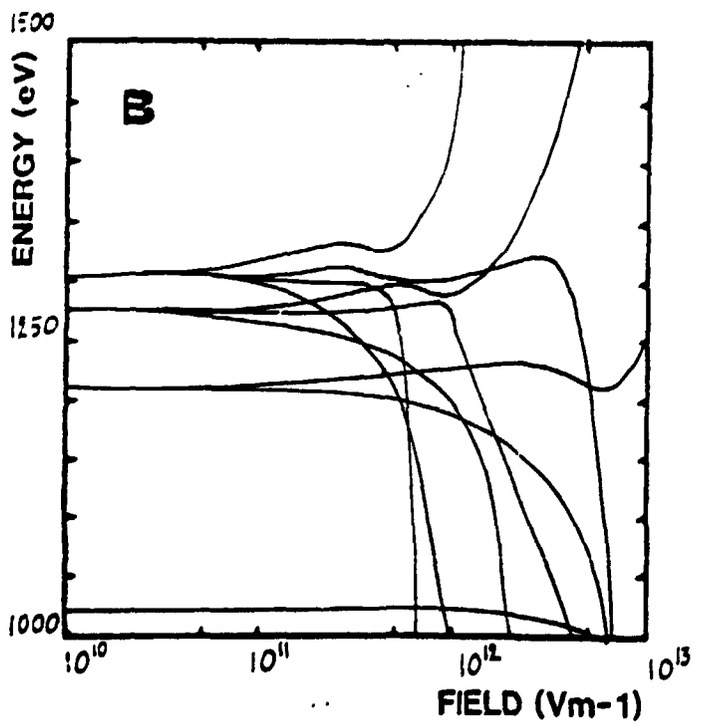
1500
ENERGY (eV)
B
1250
1000
10^{10}
10^{11}
10^{12}
10^{13}
FIELD (Vm-1)

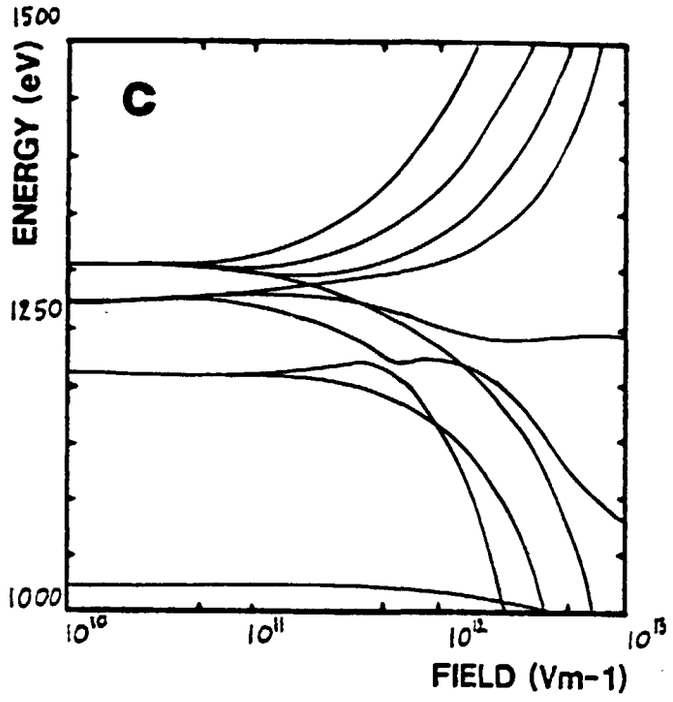

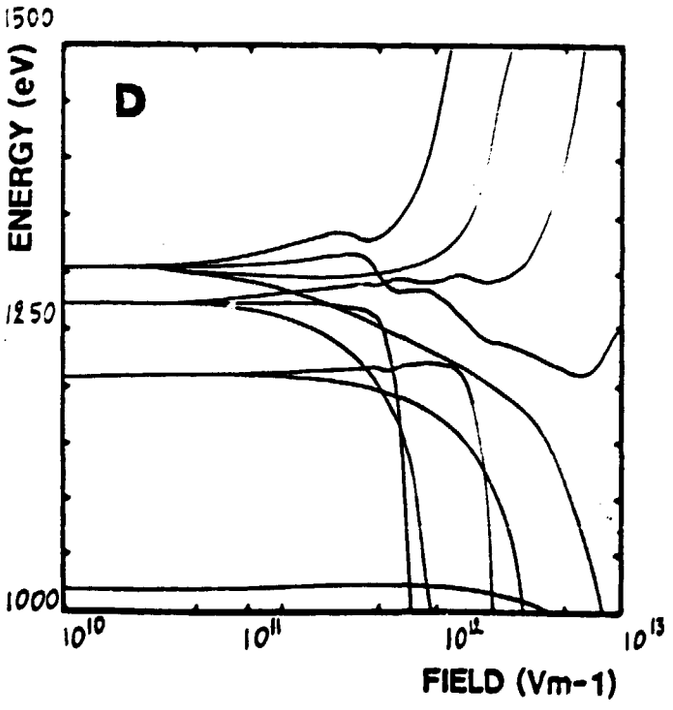

Fig. 2 : Same as Fig. 1, but for (m) = 1 states

states of different values of L_z are null

$$\forall i \qquad \langle n\, l\, m \mid V_i \mid n'\, l'\, m' \neq m \rangle = 0$$

The hamiltonian operator can then be factorized according to the values of m. We present here the results for m = 0 and m = 1 since only such states have a non zero dipolar moment with the state $|100\rangle$ ($|100\rangle$ is supposed to keep unperturbated and we checked that is really as close as possible from the numerical results we got).

7. Discussion of INN results

In the first step of n' = n terms only (A, B), the H matrix can be factorized according to the values of n and also m of course. The results are presented for the two subspaces m = 0 (fig. 1) and |m| = 1 (fig. 2) ; with the perturbating term V_1 alone (A) and with all the perturbing terms V_i (B). The solutions are calculated from the diagonalization of the submatrices (n and m fixed) of low rank (maximum 5 for n = 5, m = 0). Each one generates a set of solutions independent of the other ones. Inside a given set, there is no problem of confusion or crossing. For solutions of different sets the intersections are simple crossings without any mixing.

The problem gets more complicated when the terms connecting different values of n are introducted (C, D). The only remaining factorization is over m values, but the resulting submatrices are of a higher rank than previously (15 for m = 0, fig. 1, and 10 for |m| = 1 fig. 2) where the new energy versus field curves originate from different levels, the splitting now creating new crossings and anti-crossings. Interpreting these ones from the numerical results is quite difficult, since we have no apriori idea of their identification, and since the calculation for discrete values of F can give only dubious results as it is obvious from these two interpretations of the same calculated points (see graph A).

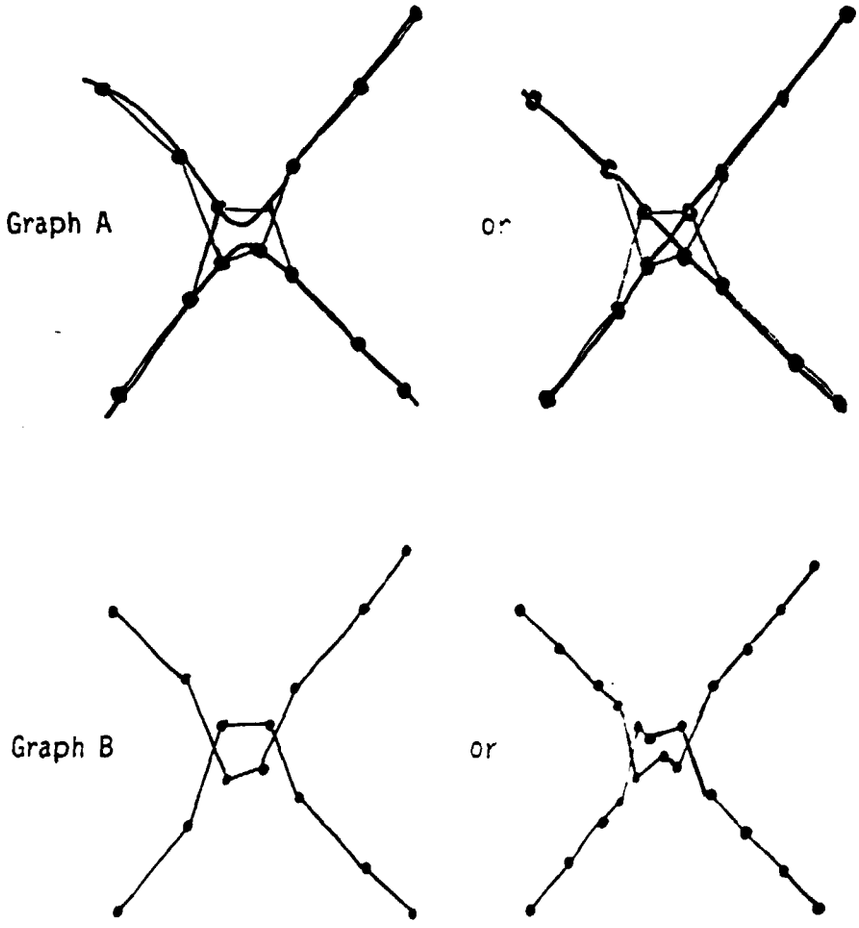

Fig. 3 : Maximal and minimal evolution of the ratio which by hypothesis is supposed laser than 1
Continuous curves = hypothesis D of Fig. 1 and 2
Dashed curves = hypothesis A of Fig. 1 and 2

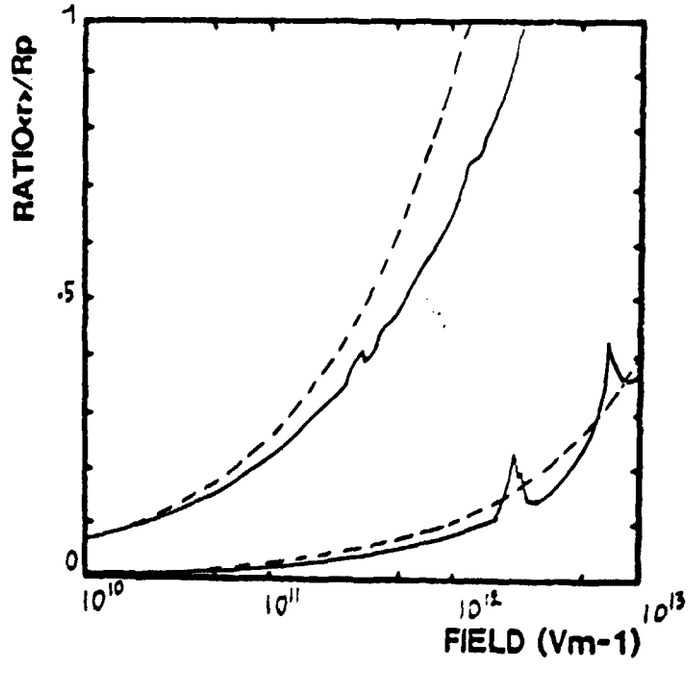

We tried different methods to solve this problem. First, the most obvious is to divide the field interval. But the confusion generally persists, as it can be seen (see graph B).

Second, we can induce a variation of the terms $n' \neq n$ while keeping the correct value of the terms $n' \neq n$. From the variation of the solutions, one ordinary can get a subjective conviction, but the automatic plotting keeps false.

Third, we tried to assume the continuity of the curves by maximizing the scalar product of the set of new eigen vectors by the set calculated with the previous value of the field. Different combinations and orders of the eigen vectors can then be tested. This method, quite expensive in computer time is correct only for little intervals between the discrete F values, or else it is unstable since some of the eigen states do exchange their components at the dubious point. It was still used to give a confirmation of the results we finally got. Fourth, the right method was proposed by our colleague C. Stavynkevitch who also wrote the relevant subroutines . For each step - consisting of a value of F - we use as projection steps not the hydrogenic solutions $|n\&m\rangle$ but the set of eigenstates $|i\rangle$ calculated at the previous step. When the new eigenstates are thus calculated, we can come back to the ordinary $\{|n\&m|\}$ basis. Since these algorithms are very fast, this method is not much slower than the diagonalization without any solutions rearrangement, because of the creation of new zero terms in the matrix, that a Jacobi solution algorithm can over pass. So we use this method for each F-step, instead of restricting the use to the step where a problem really arises.

Each crossing, resulting from an exceptionnal energy degeneracy is the effect of an additionnal casual symmetry. Then it is difficult to derive a perfect interpretation from a calculation using a projection basis so restricted ($n \leqslant 5$) that it is theoretically perfectly insufficient. But, if we restrict our analysis to the lower $n < 3$ levels it seems that we find mostly anticrossings for $m = 0$ and anticrossings for $|m| = 1$. Anyway the conclusions over the energy solutions are quite insensitive to the

limitation of the projection basis. If we compare the linear splitting A to the most complex case D, we notice that the energy positions are not so much affected. But, for the same value of F, the energy solutions to be compared do not belong to the same curves. In the case A, the eigenstates are constant. In all other cases their projections over the basis $|n\&m\rangle$ do vary with F. In the complete calculation D the effect is very important : since it governs the value of dipolar emission this is important for line shapes calculation. On the fig. 1 the n = 1 level corresponds to W = 0 for the case A.- which is quite normal - but also for the other cases B, C and D. This is not significative of the n = 1 level comportment, since we settled its energy level to zero by substracting its calculated energy level from all levels in fig. 1 and 2. As a matter of fact, since states from the continuum should be introduced into the projection basis, the real eigenstates include an evasive part by tunnel effect. We have verified that its time constant (5) is larger than our phenomena. But since there should be this mixing between free and bound states, the energy W = 0 for motionless free electrons has no real signification. Since for all atomic calculations one needs energy of the non excited state, fixing n = 1 energy equal to 0 generally is the best choice.

The last point must be the verification of our hypothesis $R_p > \langle r \rangle$. We calculated $\frac{\langle r \rangle}{R_p}$ for each eigenstate, and we present the result in fig. 3 In order to make the drawing easier, only the extremal values of $\frac{\langle r \rangle}{R_p}$ have been pointed in the hypothesis D (continuous line) and C (dashed line) and thus the importance of the different V_j terms is once more demonstrated. From the curve of the maximum value of $\frac{\langle r \rangle}{R_p}$, one can derive the maximal value of the field for which the hypothesis is respected, here 3 10^{11} V cm^{-1} for pure neon.

8. The two first nearest neighbours (2NN) approximation

The hypothesis of single first nearest neighbour presents a few drawbacks. To each value of the field, it associates the position of a single perturber, creating the exceptionnal symmetry relative to the axis Oz.

So, only one single configuration is taken into account, and it is the most singular one. Besides that, the uniqueness of the perturber makes the effect of non linear terms V_i $(i > 1)$ minimum relative to all configurations. The best and simplest way to get rid of that excessive simplification is to add a second perturber. The classical probability (p) is then inadequate since to the variable $\|\vec{F}\|$ of the total field value one needs to add the ratio of modulus $\frac{F_2}{F_1}$ and the angle of their directions $(\vec{F}_1, \vec{F}_2)$ to determine the components $\vec{F}_1 + \vec{F}_2 = \vec{F}$. We shall present our results as functions of the ratio $\frac{F_2}{F_1}$, at a given value of the total field, for different values of the angle $(\vec{F}_1, \vec{F}_2)$. The most interesting positions are the three ones when the fields are parallel or orthogonal. For parallel fields the situation where both fields point in the same direction (which means the two perturbers are on the same side, and then quite near the one from the other) is statistically less probable since the repulsive electric force would separate the two ions. So we will study only the case where the two fields are partly counter balancing each other, which is more significative of the reality.

9. Two perturbers (2N), parallel fields

Since the emitter and the perturbers are on the same axis Oz, the symmetry and the conservation of the magnetic momen L_z are preserved. The hamiltonian is then still factorizable according to the value of m . Each term Vi is the additio $V_{i1} + V_{i2}$ of two terms perfectly similar to the 1NN calculation. So there is no new term but only the addition of fields using

$$F_1 - F_2 = F$$

$$\alpha = \frac{F_2}{F_1}$$

$$R_1 = \sqrt{\frac{Z_p q}{4\pi\varepsilon_0 F_1}} = \frac{1}{\sqrt{1-\alpha}} \sqrt{\frac{Z_p q}{4\pi\varepsilon_0 F}}$$

$$R_2 = \sqrt{\frac{Z_p q}{4\pi\varepsilon_0 F_2}} = \frac{\alpha}{\sqrt{1-\alpha}} \sqrt{\frac{Z_p q}{4\pi\varepsilon_0 F}}$$

An example is given for the total field 10^{11} V m^{-1} (which is lower than the INN limit $\langle r \rangle < R_p$ by a factor 3), using only the first perturbation terms V_1 and V_2 for both fields, V_2 being enough to demonstrate the non linear effects. In this calculation the terms correcting different levels $n' \neq n$ are not taken into account, and only the level $n = 3$ is presented, to make the comparison with orthogonal fields possible - see infra -. The energy solutions are very little perturbed. The degeneracies are not splitted - except an accidental one - and even the wavefunction keeps very little altered.

10. Two perturbers (2NN) orthogonal fields

We keep the field F_1 on the Oz axis, and we add F_2 on Ox axis, so that $\overrightarrow{F_1} + \overrightarrow{F_2} = \overrightarrow{F}$

$$\Rightarrow \quad F_1^2 + F_1^2 = F^2$$

The axial Oz symmetry is then no longer true, and therefore there is no longer a factorization according to m. In the perturbation matrix

$$H = H_0 + \sum_i V_i$$

$$V_i = V_{i1} + V_{i2}$$

$$V_{i1} = -\frac{Z_{P1}\, q^2}{4\pi\varepsilon_0 R_{P1}} \left(\frac{r}{R_{P1}}\right)^i Y_i^0(\theta, \varphi)$$

$$V_{i2} = -\frac{Z_{P2}\, q^2}{4\pi\varepsilon_0 R_{P2}} \left(\frac{r}{R_{P2}}\right)^i Y_i^0(\Xi, \Phi)$$

(Ξ, Φ) being defined by :

$$\cos \Xi = \sin\theta \cos\varphi$$

$$\sin \Xi = \sqrt{1 - \sin^2\theta \cos^2\varphi}$$

$$\cos \Phi = \frac{\sin\theta \sin\varphi}{\sqrt{1 - \sin^2\theta \cos^2\varphi}}$$

$$\sin \Phi = \frac{\cos\theta}{\sqrt{1 - \sin^2\theta \cos^2\varphi}}$$

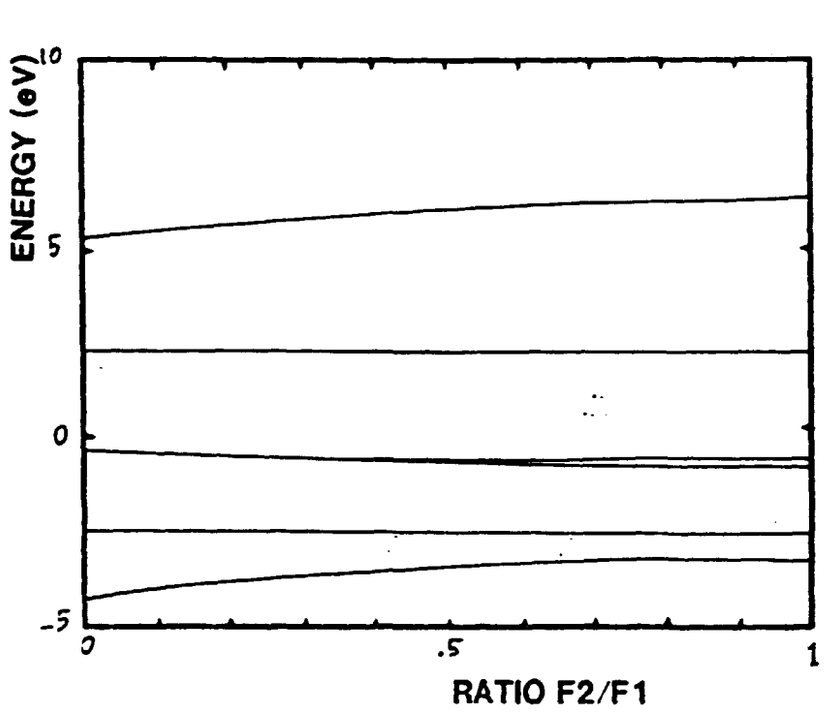

Fig. 4: Eigen energies evolution versus the ratio of two parallel fields
The hypothesis correspond to ref. (6)

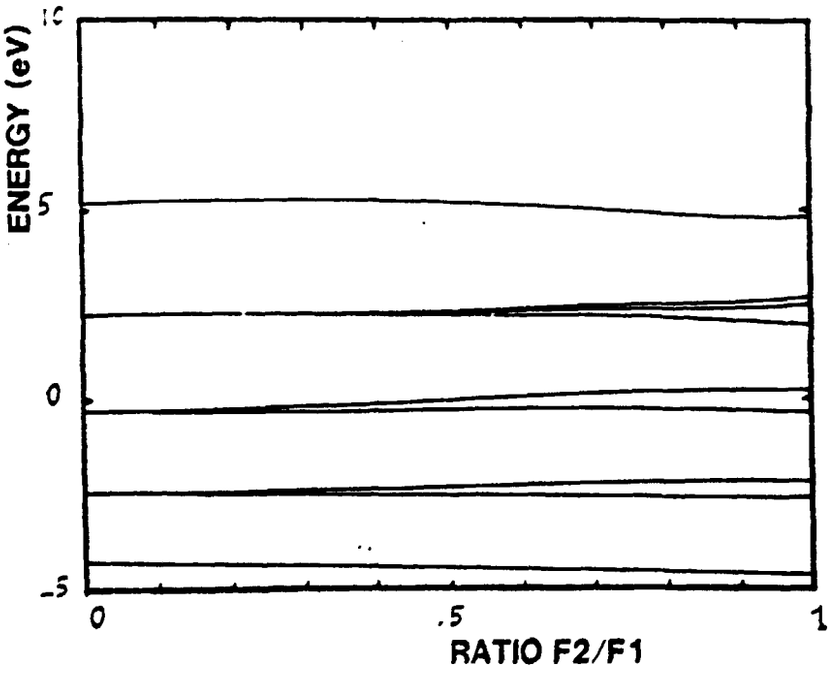

Fig. 5 : Same as Fig. 4, but for two orthogonal fields

and, with $\frac{F_2}{F_1} = \alpha$, (R_{P_1}, R_{P_2}) being defined by :

$$R_{P_1} = \sqrt{\frac{Z_{P_1} q}{4\pi\varepsilon_0 F_1}} = \frac{1}{(1+\alpha^2)^{1/4}} \sqrt{\frac{Z_{P_1} q}{4\pi\varepsilon_0 F}}$$

$$R_{P_2} = \sqrt{\frac{Z_{P_2} q}{4\pi\varepsilon_0 F_2}} = \frac{\alpha^{1/2}}{(1+\alpha^2)^{1/4}} \sqrt{\frac{Z_{P_2} q}{4\pi\varepsilon_0 F}}$$

As in all previous calculations, the new perturber terms are calculated while extending the use of the form $\text{Min}\left(\frac{r}{R_P}, \frac{R_P}{r}\right) = \frac{r}{R_P}$ even outside the sphere of radius R_p. As they were due to, these new terms now connect states $|nlm\rangle$ of different magnetic projections, and the perturbation matrix cannot be factorized. If we want to use a projection basis including all hydrogenic states up to n = 5 level, that means the matrix rank is now 55 - since we can ignore the spin projection - and for each term V_{i2} as much as 1540 coefficient could appear (even using the Hermite symmetry) which for i being limited between 1 and 8, and all limitations taken into account, would mean about 4000 new terms to calculate !

Whose the reader will accept this evaluation as a convincing excuse for not to present a calculation including all these terms. Anyway, the numerical solution would be far too long, and the resulting diagrams would be too confused to be understandable. That is the reason of the restriction to the 9 x 9 matrix dealing with the level n = 3 only, and to the use of perturbing terms V_1 and V_2 only. The results are presented fig. 5 for the same conditions as for fig. 4 of parallel fields - this explaining the unnecessary restriction of § 9 -. The degeneracies are now splitted but eigen energies and even eigenstates do not differ very much from 1NN calculation.

One must remember that whereas the axial Oz symmetry is broken by the introduction of a second perturber on Ox, the configuration keeps the simpler planar zox symmetry. This is perhaps the explanation of a special feature we noticed in the perturbation matrix $H = H_0 + V_1 + V_2$ for the level n = 3. In this 9 x 9 matrix, we found an unexpected factorization into a matrix 6 x 6 dealing with the subspace of $\{|300\rangle, |31\text{-}1\rangle, |31\text{+}1\rangle, |32\text{-}2\rangle, |320\rangle, |32\text{+}2\rangle\}$ and a 3 x 4 matrix dealing

with {|310>, |32-1>, |32+1>}. Each subspace presents the particularity that, for a given value of orbital moment, it connects one state to the others of same parity of m. It would be interesting to test whether this factorization keeps true :

- for other terms V_i, $i > 2$;
- when states of different principal quantum numbers are connected.

To break the remaining planar xoz symmetry one could add a third perturber (3NN) on Oy axis for example. But this configuration, too, is not representative of reality, since the hypothesis of three perturbers neatly closer to the emitter than any other, and thus very close to it, is unlikely, particularly since they would be in the same octant = 1/8° of space, regardless of ion repulsion. Since the energy levels - and even the eigen states - are less affected than we thought by the second perturber, the action of a third is likely unimportant.

11. Conclusions

Even without completion, the resolution of the two nearest neighbours hamiltonian enabled us to achieve the very important conclusion ... that the second perturber is of little importance. Even if this conclusion is less rewarding for our calculations than expected, it does valid the common use of 1NN calculation, which is more usable anyway. In this 1NN hypothesis, we tried to better acknowledge the perturber precise effect by the expansion $\sum_i V_i$ of the Coulomb potential, and to acknowledge the electronic states nature by the extension of the representative projection basis. The first point was investigated by the arithmetical exact calculation, but with the single expression $\mathrm{Min}\left\{\frac{\pi}{R_p}, \frac{R_p}{\pi}\right\} = \frac{\pi}{R_p}$. A more complete presentation of the individual effect of each V_i will follow in another paper.

Second, we got rid of the restriction to the single n projection states restriction. The general position of the splitted new eigen energies is not much modified, but the continuous evolution versus F is quite a

surprise, presenting many extrema. Since the line profile uses the ratio $\left(\frac{\Delta W_i}{\Delta F}\right)^{-1}$ (6), this last point is very important. Another reason for such importance is the fact that eigen states $|i\rangle$ which were little emitting previously, because their projections over the $|n\,1\rangle$ and $|n\,1 \pm 1\rangle$ states were low can now have a more important dipolar strength because there appear new useful projections over $|n \pm 1,\ 1,\ 0\rangle$ and $|n \pm 1,\ 1,\ \pm 1\rangle$. These effects mostly appear for large field values, of course, the probability of which is low. But this only means there importance lies in the wings which are better diagnosis tools since they are the lesser reabsorption regions of the spectrum. Another reason for such importance is the fact that, when n increases, corresponding lines tend to merge into a kind of continuum. With a coherent treatment of different n, the energy between the lines (which we still call "line emission", since it is bound-bound emission) can now be calculated. The evidence, now, and the calculation, soon, of this continuous emission uses these "far from the diagonal" terms, forgotten for so long and which we proved to be so important.

References

1. Griem, H., Spectral line broadening in plasmas
2. Baranger, M., Mozer, Phys. Rev. 115, 521 (59) ; 118, 626 (60), Held, B., Dissertation (Univ. of Paris Sud, 1981)
3. Hooper, C.F., Phys. Rev. 143, 77 (66) ; 165, 215 (68) ; 169, 193 (68), Tighe, R.J., Hooper, C.F., A14, 1514 (76), A15, 1773 (77) ; A17, 410(78), Tighe, R.J., PhD dissertation (Univ. of Florida, 1977)
4. Louis-Jacquet, M., to be published
5. Luc-Koenig, E., Private communication
6. Lambert, D., 5° ICSLS Berlin (1980), 14° ECLIM Palaiseau (1980)